An Efficient Hybrid Framework U-Net-based deep learning Technique of Early Detection of Pulmonary Nodules using LIDC-IDRI Dataset



Hataw Jalal Mohammed¹, Fawzi Abdul Azeez Salih², Tofiq Ahmed Tofiq³, Shaniar Tahir Mohammed³

¹Charmo Center for Research, Training, and Consultancy, University of Charmo, Sulaimani, Iraq, ²Department of Computer Science, College of Basic Education, University of Sulaimani, Sulaimani, Iraq, ³Department of Computer Science, College of Science, University of Sulaimani, Sulaimani, Iraq

ABSTRACT

Radiologists still face difficulties and mistakes while screening lung computed tomography (CT) images for pulmonary nodules, particularly small and inconspicuous malignant lesions. Frequent radiation exposure, the complexity of radiomic characteristics in low-dose CT scans, and the high cost of imaging therapy are some of the challenges. Our technique proposed a novel automated computer-aided diagnostic technique to address these issues by increasing the accuracy of early lung nodule diagnosis. We suggested a four-step technique that involves (1) a preprocessing step consisting of contrast-limited adaptive histogram equalization to refine the contrast of contribution inputs, followed by extracting and combining texture and shape features in parallel using a gray level co-occurrence matrix for the first features and region of interest (ROI) properties for the second. In addition, we suggested a hybrid U-Net-based deep learning architecture for categorization that successfully blends automatically learned features with manually created features. This integration improves the precision and resilience of pulmonary nodule classification by utilizing the convolutional neural networks (CNN)'s capacity to capture spatial hierarchies. We implemented our proposed technique on the overtly accessible Lung Image Database Consortium and Image Database Resource Initiative (LIDC-IDRI) dataset, employing the Python programming language for the implementation. Experimental results confirmed that our technique attained segmentation and classification results of 95.35% accuracy, 95.33% sensitivity, 94.23% specificity, and 95.44% AUC rates, outperforming several state-of-the-art methods. This high-performance approach offers a reliable solution for early detection, potentially reducing lung cancer mortality rates through timely diagnosis.

Index Terms: U-Net, Convolutional Neural Networks, Pulmonary Nodule Detection, Lung Image Database Consortium

1. INTRODUCTION

Pulmonary nodules cancer in its primary phases is not evident with obvious symptoms, which impede early diagnosis [1].

Access this article online

DOI:10.21928/uhdjst.v9n2y2025.pp266-275

E-ISSN: 2521-4217 P-ISSN: 2521-4209

Copyright © 2025 Mohammed, et al. This is an open access article distributed under the Creative Commons Attribution Non-Commercial No Derivatives License 4.0 (CC BY-NC-ND 4.0)

Published statistics indicate that lung nodule cancer is an important role of the leading reasons of destruction of the living in the world, accounting for 18.75% of wholly cancer deaths [2]. Furthermore, according to a study conducted in 2023, more than 238,000 people in the United States are expected to be exposed and diagnosed with lung cancer, and nearly 127,000 lung cancer patients will perish [3] and according to a study conducted in the following year, the facts indicated that about (50%) of smokers suffer from a lung nodule, and (25%) suffer from two or more [4]. Since pulmonary nodules are small spots in the lung tissue

Corresponding author's e-mail: Hataw Jalal Mohammed, Charmo Center for Research, Training, and Consultancy, University of Charmo, Sulaimani, Iraq. Email: hataw.jalal@chu.edu.iq

 that are solider than the surrounding lung, they are usually sphere-shaped or oval, furthermost of these nodules are smaller than 1cm in size, while they can grow up to 3cm in size, trials by organizations such as the National Lung Screening Trial (NLST) have indicated the high sensitivity of (CT) which can help stakeholders detect lung cancer early and thus reduce lung cancer deaths by (20%) [2]. Since it can effectively help doctors recognize the size, shape, and nature of pulmonary nodules more accurately by making it easier to identify important features present in each imaging slice such as texture and shape [4], the early diagnosis of nodules is very necessary for the controlling of lung cancer affected [5]. Fig. 1 illustrates how pulmonary nodules from a well-known open-source image dataset which they may be spherical opacities or irregular lung lesions ranging in size (3–30) mm and can be hermitic or multiple.

Nodules usually have various kinds and morphologies [6] such as (with/without) vasculature attachment (surrounded/not surrounded) by vasculature and lung membrane, (Far/near) to the diaphragm, (regular/irregular) formed, (low/high) contrast nodule, (has/has not) vasculature attachment, (single/multiple) in number, boundaries (smooth/rough), density (solid/semi solid/ground glass) nodule, and position (specified/unspecified)) as shown in Fig. 2.

Simultaneously, computer-aided diagnostic (CAD) is a typical technique as a domain of digital image processing for recognizing and detecting the many-sidedness of diseases, as well as different kinds of cancer. Moreover, it's systems also provide appropriate support for clinical decision-making [7]. The majority of pulmonary nodule detection systems perform two tasks: Lung nodule detection

techniques achieve two missions: (1) Detect candidate nodules and (2) reduce false positives (FPs). Any nodule not determined at initial stage will no far be retrieved later. Thus, the first stage typically permits to be actual very sensitivity in being evident with the rate of numerous FP cases. Consequently, the second phase aims to reduce the number of FPs [8]. In recent years, CAD systems have mainly depended on machine learning (ML) and deep learning (DL) technologies [9], which introduce a major role as a second interpreter in the interpretation of CT images [4]. The aim of choosing DL is to eliminate the major drawbacks of using traditional ML methods, especially when it depends on feature extraction [9]. In spite of DL requiring large amounts of computing power and data for training, it has been widely researched due to the accuracy of its estimations [7]. DL has proven itself as a major breakthrough not only in the fields of medicine but also in another numerous scientific fields, making far-reaching changes in the way we learned and interpreted complex data forms. Enclosed by the dominance of medical imaging, mainly in the analysis of CT lungs, there is an eminent tendency where DL models are being combined for nodule segmentation. These models involve numerous network architectures such as convolutional neural networks [CNNs] which are the furthermost broadly used, VGG16, ResNet [10], dual-branch residual networks, Mask R-CNN, and U-Net [3].

A full decade has passed since the invention of U-Net and its assistance in the field of medical image processing [11] as a semantic segmentation network built on a fully CNN [12]. Its manner was developed as a product of the development and enhancement of CNNs. In addition of allowing computing the measurable attribute of damaged (texture, perimeter,

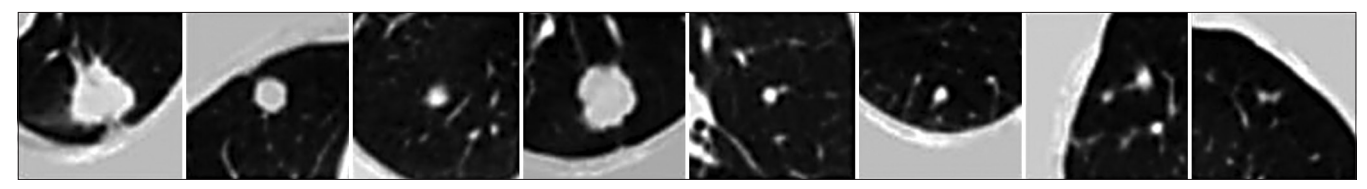


Fig. 1. Computed tomography image examples of the dataset (lung image database consortium).

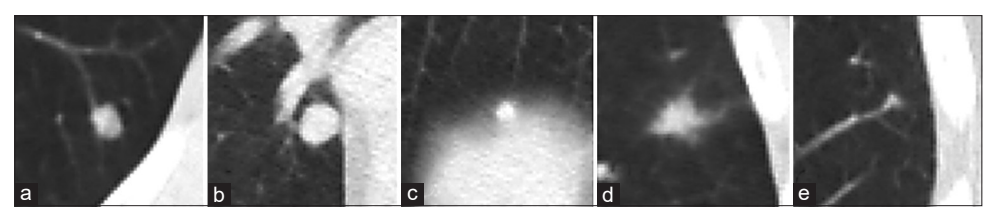


Fig. 2. Various kinds of pulmonary nodules. (a) With vasculature attachment. (b) Between vasculature and lung membrane. (c) Small and near the diaphragm. (d) Irregular shape with low contrast. (e) Has not vasculature.

direction, area, etc.), which facilitates the identification of the nature of the damage and improves and reduces the treatments required to exclude it [11].

The basic U-Net neural network structure is a typical convolutional network construction consists of repeated application of convolutions, each followed by a rectified linear unit (ReLU) and a max pooling, gives a symmetric U-shaped architecture as indicated in Fig. 3, as noted that it consists of dual parts: The left is the compression (encoder) and the right is the expansion (decoder). Throughout the reduction, the spatial information is decreased while feature information is increased. The extensive pathway collects the feature and spatial information through a sequence of up-convolutions and concatenations with high-resolution features from the constraining path.

At the termination of each up-sampling, convolution is applied consuming a (3×3) kernel and a ReLU activation occupation. During the up-sampling process, new pixels are increased until the input is molded as the desired dimension, allowing the last layer to utilize a (1×1) convolution which aligns feature vectors to the aim classes.

Building a hybrid U-Net-based DL framework for the lung image database consortium (LIDC)-IDRI dataset's early pulmonary nodule identification and classification is the goal of this research. Through the integration of strong segmentation and classification approaches designed to identify nodules early on, the goal is to increase diagnostic accuracy by utilizing DL's advantages in medical image processing.

2. RELATED WORK

Over the earlier years, cancer handling has been the serious emphasis of medical research on human health over the world [13]. In this section, we presented a comprehensive review of the research conducted over the last decade that has focused on the same subject as our study. Sun et al. in 2016 [14], introduced another study using CNNs. The authors implemented three distinct DL approaches, utilizing cropped (52 × 52) pixel covers from the LIDC dataset for training and testing. These approaches included CNN, deep belief networks (DBN), and a stacked denoizing autoencoder (SDAE). The CNN model featured 3 convolutional layers, each followed by max pooling, using 5×5 kernels to produce (6, 8, and 12) feature maps. Nodule areas in the images were segmented based on the uniting form of truth files from 4 radiologists. Accuracy was relied upon in performance evaluation, with CNN, DBN, and SDAE achieving scores of 79.76%, 81.19%, and 79.29%, respectively.

In Zhang et al. [15] developed a globally optimized hybrid geometric active contour model along with a computerized lung segmentation technique, by integrating both global sections and edge information, the algorithm achieved a very high and average F-measure of (99.22%). The efficiency of the algorithm was validated on (40) images of CT scans from the LIDC dataset. In (2018) Sindhu et al. [16], employed a single CNN that instantaneously predicts multiple bounding boxes and their corresponding class probabilities. The approach combined object classification and regression to estimate bounding boxes, resulting in higher inference performance compared to standard classifiers used with a

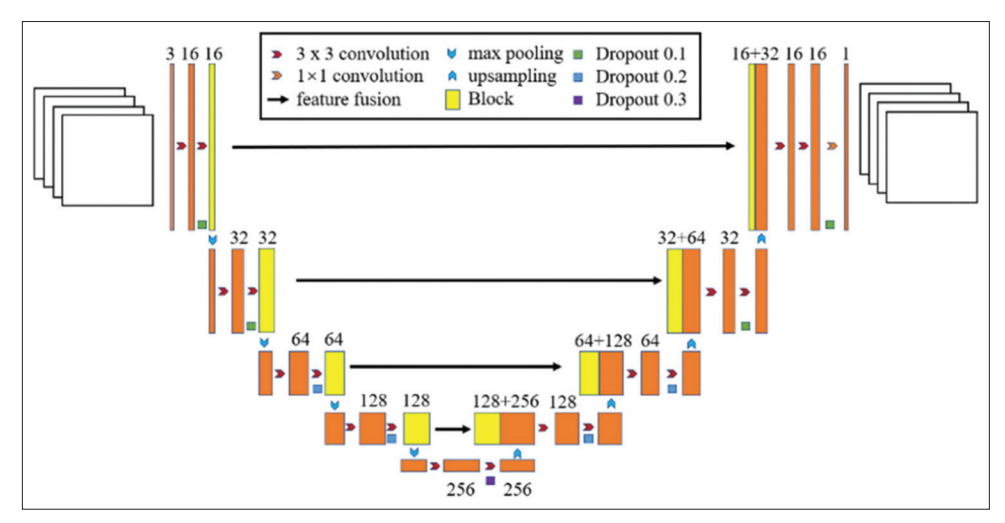


Fig. 3. General structure of the U-Net neural network.

sliding window approach. The Detect-Net model featured a 22 fully convolutional layers without any fully connected (FC) layers, enabling the network to admit the inputs of varied sizes and apply the CNN in a sliding window style with suitable paces. The system was evaluated on the LIDC dataset and achieved a sensitivity of 89% at 6 FPs per image and a precision of 93%. Xie et al. [17] modified the faster R-CNN framework by integrating two region proposal networks and a deconvolutional layer to reveal nodules expected. They trained (3) separate models for several types of slices, which were later fused to produce the final results. In addition, they introduced a 2D CNN-based boosting architecture for FP reduction, functioning as a classifier to differentiate true nodules from candidates. Misclassified samples were retained for retraining, improving sensitivity for pulmonary nodule detection. The final categorization results were gained through a voting process that combined the outputs of these networks. Extensive testing showed that a sensitivity of candidate detection was 86.42%. Qinhua et al. (2020) developed another technique using an automated segmentation of the lungs in CT images, used mask R-CNN, to specify the model for region mapping of the lung, incorporated with supervised and unsupervised ML methods Bayes. The technique obtained an additional accurate response related to the benchmarked approaches, with a segmentation accuracy of 97.68% [18]. Masood et al. [19] introduced an improved multi-dimensional regionbased fully convolutional network approach for detecting and classifying pulmonary nodules using LIDC-IDRI dataset. By means of incorporating an efficient multi-layer fusion region proposal network with spatially-sensitive score maps as the cornerstone of the image classifiers, the authors utilized a median intensity projection to leverage CT scan data with applying a deconvolutional layer to identify areas of interest. When compared to other detection and classification methods, the system reached a rate of sensitivity (98.1%) and (97.1%) of accuracy.

After a year, Gopi *et al.* [20] suggested a technique for categorizing and confirming the reliability of different phases of pulmonary nodules progression and introduced a Cloud-based Lung Tumor Detector and Stage Classifier (Cloud-LTDSC) as a hybrid technique for analyzing positron emission tomography/CT images. They used the LIDC-IDRI benchmark dataset and assessed an experimental efficiency result (98.6%) as a rate of classification accuracy.

Musthafa et al. [21] proposed a hybrid ML technique for early lung nodule prediction from the LIDC-IDRI dataset using

a neural network-based approach for classification. Their approach integrated multiple machine learning methods, including support vector machine, Mask-Region-based Convolutional Neural Network (RCNN), and CNNs, and they introduced an improved snake swarm optimization with a bat model that used statistical data. In addition, a chaotic atom search optimization algorithm was applied to choose the most relevant features, reducing the dimensionality problem. Finally, they designed a learning-based deep neural network hybrid classifier for nodule detection and gained (96.39%), (95.25%), (96.12%), and (96.05%) of accuracy, sensitivity, specificity, and area under the curve (AUC), respectively.

In the same year, Konovalenko et al. [11] proposed U-Net-like architectures using encoders such as ResNet, DenseNet, and others and investigated the relevance between the training validation measurements and the final segmentation test. After analysing the detection accuracy, they found that neural networks trained consuming Nesterov momentum stochastic gradient descent optimizer had the greatest generality properties. To choose the superlative model throughout training based on the validation measurements, the core test measurements of recognition quality (dice similarity coefficient) were analyzed based on the validation metrics. It was found that ResNet and DenseNet models realize the highest generalization characteristics for their task. The maximum accuracy for recognition was achieved using the ResNet152 backbone with U-Net model. Their proposal reached 93.04% of accuracy.

After a year, Suriyavarman *et al.* combined an efficient net neural network technique with U-Net for both goals (segmentation and classification) of pulmonary nodules on the LIDC-IDRI dataset. A semi-supervised technique that depends on extracting features was used to yield the advantage of the massive amount of input images without extreme signs. They applied ResNet-50 model and feature pyramid network (FPN) to extract features and then applied a neural network classifier to estimate unlabeled nodules. Their technique's results presented a higher accuracy of (91.67%) [22].

Gupta et al. proposed framework exploited an adapted U-Net architecture on the LIDC-IDRI dataset which employed the classical u-net manner for multi-scale feature extraction with Differentiable Architecture Search (DARTS) which applied perception of effective architecture illustration. Moreover, the adapted U-Net is accomplished detecting and classifying pulmonary nodules efficiently also professionally. The proposed framework obtained 95.01% of accuracy rate [23].

The related works covered in this part are summarized in Table 1 below, it should be noted that numerous other studies have also used the LIDC-IDRI dataset and produced encouraging results, but a thorough discussion of those studies was not possible owing to space constraints.

Our suggested methodology has a number of advantages over other methods, such as better classification performance by integrating handmade and deep features, more robustness in recognizing small or low-contrast nodules, and more accurate segmentation thanks to the U-Net design. This hybrid approach, in contrast to conventional techniques, combines DL and feature engineering, leading to improved generalization and increased diagnostic accuracy on the LIDC-IDRI dataset.

3. PROPOSED APPROACH

This section reveals the detailed of our proposed approach which comprises the detection of pulmonary nodules using DL which has become a key motivation in medical imaging, essentially for early lung cancer diagnosis. It is also worth mentioning that several DL techniques are extensively used and have been confirmed to be effective. The preferred approach is often contingent on the dataset, computational properties, and the accuracy required.

In this study, we proposed a hybrid image classification approach combining texture and shape feature extraction methods with (U-Net CNN) to classify the LIDC images into two predetermined kinds. The method consisted of numerous phases: Preprocessing, features extraction, and u-net-based DL classifications as shown in Fig. 4 bellow.

Our workflow can be summarized as follows:

3.1. Dataset Preparation

LIDC resource is an open-accessible universal dataset for the development and evaluation of CAD approaches to pulmonary nodules detection and diagnosis, which contains (1018) medical CT scan images and an associated XML [24]. Each image was labeled for pests that belonged to one of three classes ("nodule >=3 mm," "nodule <3 mm," and "non-nodule >=3 mm"), and the aim of this idea is to recognize as completely as possible all nodules for each image in the dataset [25].

3.2. Preprocessing

Our preprocessing techniques were used to enhance the feature of the images, which in turn improve the performance of the

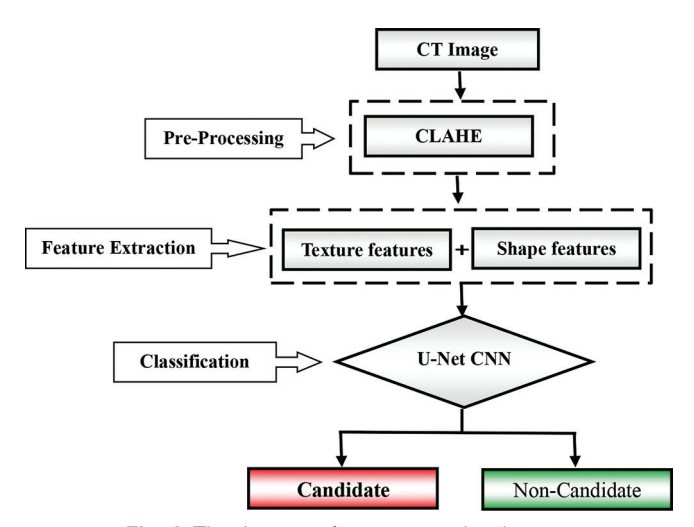


Fig. 4. The diagram of our proposed technique.

detection and classification, by enhancing the contrast of specific ranges after adjusting the intensity levels according to local histograms [26], this stage involved the contrast limited adaptive histogram equalization (CLAHE) algorithm as shown in Fig. 5, which executed to enhance the contrast of each input image.

3.3. Texture and Shape Feature Extraction

The step before applying the DL model, we preferred to employ both texture and shape-based feature extraction techniques to support the U-Net's performance:

- a) Texture Features: Gray-level co-occurrence matrix (GLCM) algorithm is computed from grayscale images to capture the texture details. GLCM is computed with an offset of [0, 1] and a specified some of gray levels to encrypts information about the spatial relationship between pixel densities and depicts important texture patterns, and seven texture features had been extracted, which capture different aspects of the texture of each image, and the features were Contrast, Correlation, Energy, Homogeneity, Entropy, Dissimilarity, Autocorrelation.
- b) Shape Features: After applying Otsu's segmentation to the preprocessed image to obtain a binary mask, we extracted four shape-based features using the region prop's function included (Area, Perimeter, Eccentricity, and Solidity) were merged, respectively, into a single feature vector that is ultimately appended to the seven texture features extracted from GLCM to estimate the performance of the classification.

3.4. U-Net-based Architecture

Our technique is performed using a hybrid approach, where both texture and shape features are combined with features

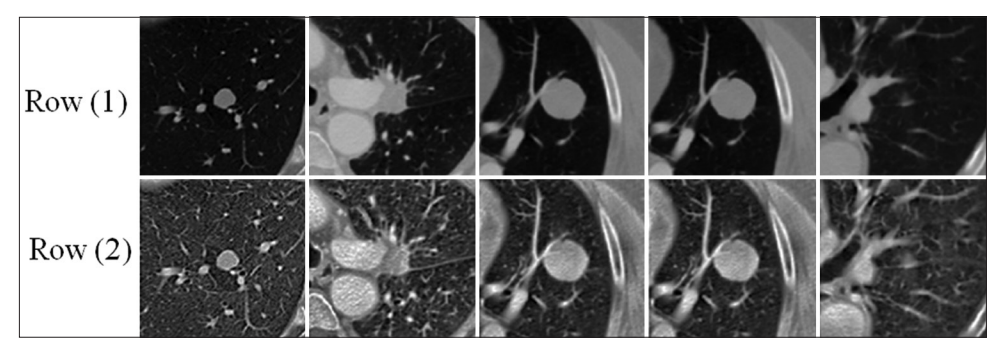


Fig. 5. Demonstrates the differences between the original images row (1) and the same images after applying contrast-limited adaptive histogram equalization row (2).

| Author (s)/year | Preprocessing | Model training/network | Feature Extraction | Classification | Results % |
|--------------------------------------|--|---|---|--|---|
| Sun <i>et al</i> .[14] in 2016 | Cropped patches (52×52), truth file segmentation | CNN, DBN, SDAE with 3 conv layers each | CNN feature maps (5×5 kernels) | CNN/DBN/ SDAE classifiers | Accuracy CNN: 79.76 DBN: 81.19 SDAE: 79.2 |
| Zhang <i>et al</i> .[15] in 2017 | Lung segmentation | Hybrid geometric active contour | Global and edge info | N/A | F-measure: 99.22 |
| Sun <i>et al</i> .[16] in 2018 | N/Ă | Detect-Net (22 conv layers, no FC) | Bounding box regression+ classification | Sliding window with detection model | Sensitivity: 89 Precision: 93 |
| Xie <i>et al</i> .[17] in 2019 | N/A | Modified faster R-CNN with two RPNs | 2D CNN-based boosting, deconvolutional layer | Voting-based classifier | Sensitivity: 86.42 |
| Qinhua <i>et al.</i> [18] in 2020 | Mask R-CNN-based lung segmentation | Supervised+unsupervised machine learning+Bayes | Region mapping | Bayes classifier | Accuracy: 97.68 |
| Masood <i>et al</i> .[19] in 2020 | Median intensity projection | multi-dimensional region-based fully convolutional network with multi-layer fusion region proposal network, deconvolutional layers | Spatially-sensitive score maps | Region-based FCN | Sensitivity: 98.1 Accuracy: 97.1 |
| Gopi <i>et al.</i> [20] in 2021 | N/A | Cloud-based lung tumor detector and stage classifier with positron emission tomography/CT integration | N/A | Multi-phase hybrid classifier | Accuracy: 98.6 |
| Musthafa et al.[21] in 2022 | Statistical feature selection | Hybrid machine learning: Support vector machine, Mask-RCNN, CNN, improved snake swarm optimization with a bat model, CASO | CASO for best features | Learning-based deep neural network hybrid neural classifier | Accuracy: 96.39 Sensitivity: 95.25 area under the curve: 96.05 |
| Konovalenko et al.[11] in 2022 | N/A | U-Net with ResNet/DenseNet encoders | Nesterov SGD training | ResNet152 with U-Net | Accuracy: 93.04 |
| Suriyavarman et al.[22] in 2023 | Semi-supervised learning on unlabeled data | EfficientNet+U-Net+FPN+ResNet-50 | FPN | Neural network classifier | Accuracy: 91.67 |
| Gupta <i>et al</i> .[23] in 2024 | Classical U-Net pipeline | Adapted U-Net with DARTS architecture | Multi-scale feature extraction | End-to-end classification | Accuracy: 95.01 |

CASO: Chaotic atom search optimization, FPN: Feature pyramid network, CNN: Convolutional neural network, DBN: Deep belief network, SDAE: Stacked denoizing autoencoder, RPN: Region Proposal Networks, SGD: Stochastic Gradient Descent

learned by a custom U-Net-based. The U-Net architecture is designed specifically for medical image segmentation and classification, as detailed in Fig. 6 below:

The methodology increased model interpretability, which is essential in clinical practice, in addition to improving detection accuracy for small and subtle nodules. All things

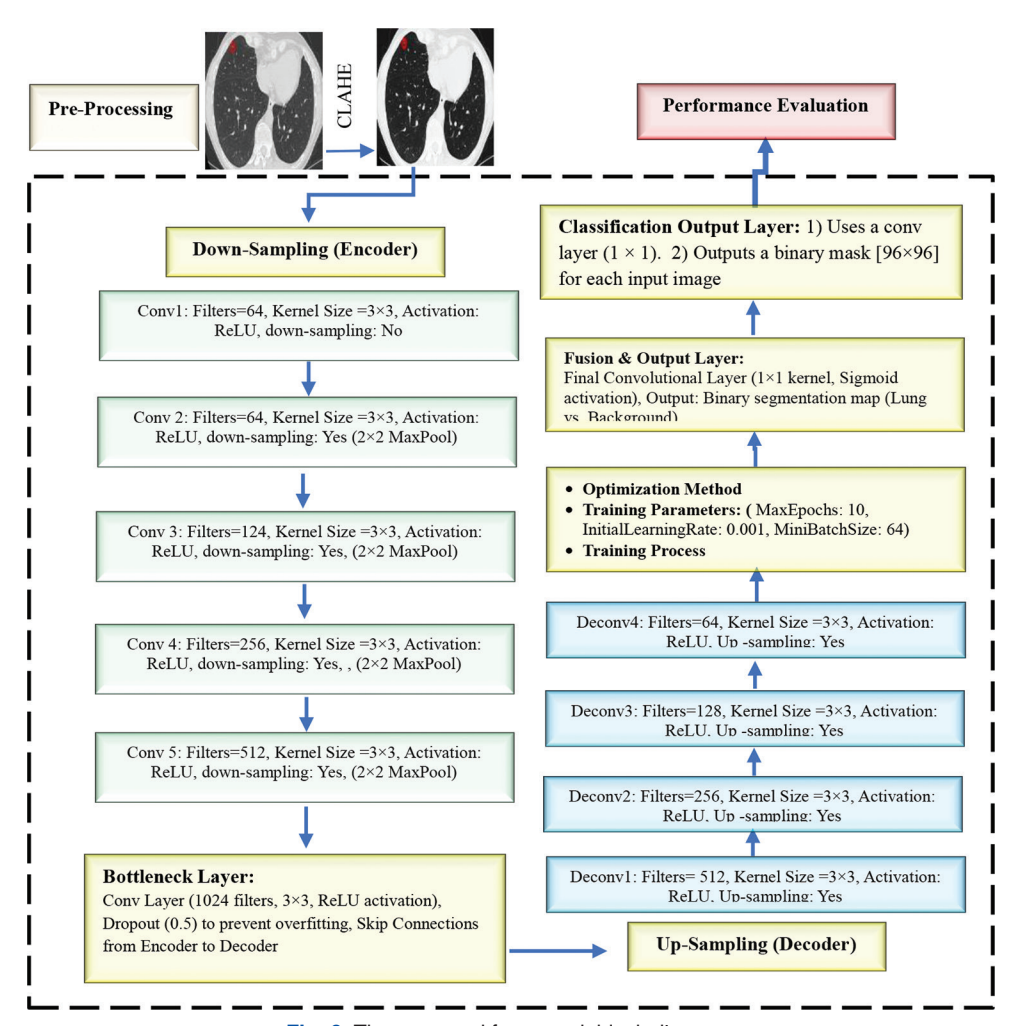


Fig. 6. The proposed framework block diagram.

considered, the framework offers a significant advancement in the direction of more accurate, comprehensible, and effective CAD in lung cancer screening.

4. EXPERIMENTAL RESULT

To compare the results with other models and decide how to use them in the future, it is standard procedure to evaluate the outcomes after an experiment [26]. We utilized accuracy, sensitivity, specificity, and AUC as metrics to evaluate the model and our methodology. The following techniques are employed to describe them:

a) Accuracy is the most commonly used measure to answer the question, "Of all the predictions we made, how many were correct?" It is the ratio of accurate forecasts to total predictions and is calculated with the use of Equation (1)

$$Accuracy = \frac{TP + FP + TN + FN}{TP + FP + TN + FN} \times 100 \tag{1}$$

b) Specificity percentage of true negative situations that were accurately forecasted to be negative. and determined using Equation (2).

$$Specificity = \frac{TN}{TN + FP} \times 100 \tag{2}$$

c) Sensitivity emphasizes the model's effectiveness in producing all the favorable results. Additionally known as the "true positive rate," it provides an answer to the query, "How many of all the data points did we acceptably predict as true?" Equation (3) below is used to calculate recall.

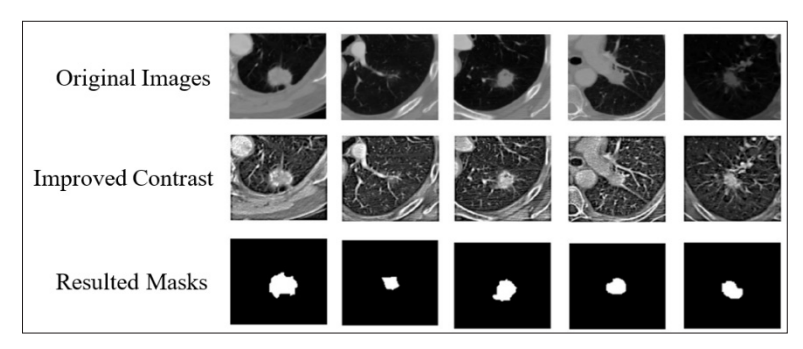


Fig. 7. Pulmonary nodule segmentation results using U-Net convolutional neural network.

| Table 2: Comparative five experimental models results | | | | | | | | |
|---|-----------|--------------|--------------|-------|--|--|--|--|
| Model | Accuracy% | Sensitivity% | Specificity% | AUC% | | | | |
| FCN | 94.32 | 94.32 | 93.30 | 93.36 | | | | |
| SegNet | 94.20 | 94.21 | 93.21 | 93.27 | | | | |
| ResNet | 94.67 | 94.67 | 93.65 | 93.71 | | | | |
| DenseNet | 95.09 | 95.09 | 94.07 | 94.13 | | | | |
| U-Net | 95.35 | 95.33 | 94.23 | 95.44 | | | | |

Sensitivity =
$$\frac{TP}{TP + FN} \times 100$$
 (3)

d) AUC, or more precisely, the receiver operating characteristic curve. It measures a binary classifier's total capacity to discriminate between positive and negative classes at every classification threshold. Equation (4) is used to determine the AUC.

$$AUC = \int_{0}^{1} TPR(FPR)d(FPR) \times 100$$
 (4)

Where TPR is true-positive rate =
$$\frac{TP}{TP + FN}$$
 (5)

and FPR is false-positive rate =
$$\frac{FP}{FP + TN}$$
 (6)

The decision to employ these particular metrics (accuracy, specificity, sensitivity, and AUC) depends on the classification challenges, the application domains, and the requirements for a thorough assessment [23].

4.1. Experimental Setup

In this study, we divided all the downloaded image in LIDC as two categories: training and testing groups, and different ratios were tested as the following (training-testing) order: (50% - 50%), (60% - 40%), (70% - 30%), then (80% - 20%); finally, we had reached that the last allocation (80% - 20%) provides the best findings.

| Table 3: Results of other comparable techniques | | | | | | | | |
|---|---------------|------------------|------------------|----------|--|--|--|--|
| Techniques | Accuracy % | Sensitivity % | Specificity % | AUC % | | | | |
| Musthafa et al. [21], 2022 | 96.39 | 95.25 | - | 96.05 | | | | |
| Konovalenko et al. [11], 2022 | 93.04 | - | - | - | | | | |
| Suriyavarman and Annie [22], 2023 | 91.67 | - | - | - | | | | |
| Gupta <i>et al</i> . [23], 2024 | 95.01 | - | - | - | | | | |
| Proposed approach | 95.35 | 95.33 | 94.23 | 95.44 | | | | |

4.2. Data Preprocessing

To improve the performance of preprocessing by adopting CLAHE to improve the input images contrast and certainly increases the accuracy and speed of nodule identification and reduce the computational load of network training and evaluation, therefore, to reduce the interference of unimportant lung regions processed on the evaluation outcomes, the obvious salient locations of each labeled image were cropped based on the node position provided in the annotation files, and the original image sizes were cropped to (96 × 96) pixels to retain the fully important private information as shown in Fig. 7.

4.3. Results

To validate our technique and ensure the segmentation effect of the proposed hybrid U-Net framework model, six models, including FCN, SegNet, Resnet, Densenet, and U-Net, were tested, respectively; the results in Table 2 showed the strength of our proposed model.

Even though the objective of this study was diagnostic accuracy, processing time is still an important consideration for real-time clinical applications. In subsequent studies, we want to assess and improve the framework's computational effectiveness. This will facilitate its useful implementation in medical situations where time is of the essence.

4.4. Comparative Analysis

More tests were conducted to evaluate our suggested technique performance by comparing it with other techniques [Table 3]. Some of cells are left as blank because all of the most recent methods either tested their strategy only in terms of accuracy or combined accuracy with other metrics.

5. CONCLUSION

Pulmonary nodules early detection using CAD systems is crucial in reducing lung cancer mortality rates, especially given the asymptomatic nature of the disease in its early stages.

In order to detect and classify pulmonary nodules early on, we used the LIDC-IDRI dataset to propose a robust hybrid DL system based on the U-Net architecture. To detect even subtle or irregular nodules, the framework showed good accuracy and reliability by combining DL approaches with efficient preprocessing, segmentation, and custom feature extraction.

Great diagnostic performance was demonstrated by the model's remarkable 95.35% accuracy, 95.33% sensitivity, 94.23% specificity, and 95.44% AUC. These outcomes demonstrate the value of integrating DL with conventional techniques to produce an all-encompassing and interpretable system. In addition to increasing diagnostic confidence, the suggested method aids in clinical judgment when screening for lung cancer. Although encouraging, additional validation on external datasets is required to improve generalizability. However, this structure provides a solid basis for further developments in automated pulmonary nodule identification.

REFERENCES

- [1] H. Jin, C. Yu, Z. Gong, R. Zheng, Y. Zhao and Q. Fu. "Machine learning techniques for pulmonary nodule computer-aided diagnosis using CT images: A systematic review". *Biomedical Signal Processing and Control*, vol. 79, p. 104104, 2023.
- [2] Y. Gu, J. Chi, L. Yang, B. Zhang, D. Yu, Y. Zhao and X. Lu. "A survey of computer-aided diagnosis of lung nodules from CT scans using deep learning". *Computers in Biology and Medicine*, vol. 137, pp. 1-27, 2021.
- [3] B. Youssef, A. Alksas, A. Shalaby, A. Mahmoud, E. V. Bogaert, N. S. Algahmdi, A. Neubacher, S. Contractor, M. Ghazal, A. Elmaghraby and A. El-Baz. "Integrated deep learning and stochastic models for

- accurate segmentation of lung nodules from computed tomography images: A novel framework". *IEEE*, vol. 11, pp. 99807-99821, 2023.
- [4] Z. Zhao, S. Guo, L. Han, L. Wu, Y. Zhang and B. Yan. "Altruistic seagull optimization algorithm enables selection of radiomic features for predicting benign and malignant pulmonary nodules". *Computers in Biology and Medicine*, vol. 180, p. 108996, 2024.
- [5] X. Zhan, H. Long and J. Wu. "A semantic fidelity interpretableassisted decision model for lung nodule classification". *International Journal of Computer Assisted Radiology and Surgery*, vol. 19, pp. 625-633, 2023.
- [6] C. Wenming, R. Wu, G. Cao and Z. He. "A comprehensive review of computer-aided diagnosis of pulmonary nodules based on computed tomography scans". *IEEE*, vol. 8, pp. 154007-154023, 2020.
- [7] R. Li, C. Xiao, Y. Huang, H. Hassan and B. Huang. "Deep learning applications in computed tomography images for pulmonary nodule detection and diagnosis: A review". *Diagnostics*, vol. 12, p. 298, 2022.
- [8] Y. Ye, M. Tian, Q. Liu and H. M. Tai. "Pulmonary nodule detection using V-Net and high-level descriptor based SVM classifier". *IEEE*, vol. 8, pp. 176033-176041, 2020.
- [9] R. Mothkura and B. N. Veerappa. "Classification of lung cancer using lightweight deep neural networks". *Procedia Computer Science*, vol. 218, pp. 1869-1877, 2023.
- [10] J. Chang, Y. Li and H. Zheng. "Research on key algorithms of the lung CAD system based on cascade feature and hybrid swarm intelligence optimization for MKL-SVM". *Hindawi, Computational Intelligence and Neuroscience*, vol. 2021, pp. 1-16, 2021.
- [11] I. Konovalenko, M. Pavlo, B. Janette, P. Olegas and B. Jakub. "Research of U-Net-Based CNN architectures for metal surface defect detection". MDPI, vol. 10, no. 5, pp. 1-19, 2022.
- [12] X. Zhang, S. Kong, Y. Han, B. Xie and C. Liu. "Lung nodule CT image segmentation model based on multiscale dense residual neural network". *Mathematics*, vol. 11, no. 6, pp. 1-14, 2023.
- [13] W. Cao, R. Wu, G. Cao and Z. He. "A comprehensive review of computer-aided diagnosis of pulmonary nodules based on computed tomography scans". *IEEE Access*, vol. 8, pp. 154007-154023, 2020.
- [14] Sun, B. Zheng and W. Qian. "Computer Aided Lung Cancer Diagnosis with Deep Learning Algorithms". pp. 1-8, 2016.
- [15] W. Zhang, X. Wang, P. Zhang and J. Chen. "Global optimal hybrid geometric active contour for automated lung segmentation on CT images". Computers in Biology and Medicine, vol. 91, pp. 168-180, 2017.
- [16] S. S. Ramachandran, J. George, S. Skaria and V. V. Varun. "Using Yolo Based Deep Learning Network for Real Time Detection and Localization of Lung Nodules from Low Dose CT Scans", 2018.
- [17] H. Xie, D. Yang, N. Sun, Z. Chen and Y. Zhang. "Automated pulmonary nodule detection in CT images using deep convolutional neural networks". *Pattern Recognition*, vol. 85, pp. 109-119, 2019.
- [18] Q. Hu, L. F. Souza, G. B. Holanda, S. S. A. Alves, F. H. Silva, T. Han and P. P. Rebouças Filho. "An effective approach for CT lung segmentation using mask region-based convolutional neural networks". Artificial Intelligence in Medicine, vol. 103, p. 101792, 2020
- [19] A. Masood, B. Sheng, P. Yang, P. Li, H. Li, J. Kim and D. D. Feng. "Automated decision support system for lung cancer detection and classification via enhanced RFCN with multilayer fusion RPN".

- IEEE, vol. 16, pp. 7791-7801, 2020.
- [20] G. Kasinathan and S. Jayakumar. "Cloud-based lung tumor detection and stage classification using deep learning techniques". *Biomed Research International*, vol. 2022, pp. 1-17, 2021.
- [21] S. Musthafa, K. Sankar, T. Benil and Y. N. Rao. "A Hybrid Machine Learning Technique for Early Prediction of Lung Nodules from Medical Images using a Learning-Based Neural Network Classifier". Wiley, United States, 2022.
- [22] S. Suriyavarman and A. X. Annie. "Lung nodule segmentation and classification using u-net and efficient-net". *International Journal* of Advanced Computer Science and Applications, vol. 14, no. 7, pp. 737-745, 2023.
- [23] A. Gupta, A. Kumar and K. Rautela. "UDCT: Lung cancer detection and classification using U-net and DARTS for medical CT images". *Multimedia Tools and Applications*, vol. 84, pp. 19065-19085, 2024.

- [24] JustinKirby. "The Cancer Imaging Archive: LIDC-IDRI". Kaggle, 2022. Available from: https://www.kaggle.com/datasets/ justinkirby/the-cancer-imaging-archive-lidcidri [Last accessed on 2024 Oct 18].
- [25] Archive, The Cancer Imaging. "LIDC-IDRI|Data from The Lung Image Database Consortium (LIDC) and Image Database Resource Initiative (IDRI): A Completed Reference Database of Lung Nodules on CT Scans". National Cancer Institute, Cancer Image Program (CIP), 2020. Available from: https://www. cancerimagingarchive.net/collection/lidc-idri [Last accessed on 2024 Oct 18].
- [26] F. A. A. Salih, S. Tahir, T. Ahmed and H. J. Mohammed. "An effective computer-aided diagnosis technique for alzheimer's disease classification using U-net-based deep learning". UHD Journal of Science and Technology, vol. 9, no. 1, pp. 34-43, 2025.